Met Office
Hadley Centre

Hadley Centre Technical Note 104

Disaggregating daily accumulations of 3-hourly WFDEI-GPCC rainfall via a multiplicative cascade procedure

February 21, 2019

Ivan Paspaldzhiev, Karina Williams, Pete Falloon

www.metoffice.gov.uk

Met Office
Hadley Centre

Contents

1 Introduction

This work reviews commonly used procedures for precipitation disaggregation, aiming to critically evaluate their applicability for use in JULES and identify the most suitable procedure. The JULES use case requires a procedure that is **J1)** applicable globally, **J2)** is defensible and has some physical backing, **J3)** circumvents the need for storing large amounts of sub-daily model data, **J4)** does not add unreasonable computational expense to running the model, and (of course) **J5)** performs adequately in reproducing the statistical properties of fine-scale rainfall. Within this work, only procedures for downscaling of temporal rainfall are considered, space and space-time approaches are only briefly acknowledged. For the purposes of JULES, this is not entirely unreasonable, as therein calculations are already on a cell-by-cell basis, though the disaggregator implementation may have implications for the spatial (and temporal) autocorrelation of the data.

The three main approaches in the disaggregation literature are multiplicative cascades, point-process models and method-of-fragments (resampling-based) procedures. Point-process models represent the onset and magnitude of storms and individual storm cells as an aggregation of independent random processes [Rodriguez-Iturbe et al., 1987, 1988], which is attractive from a physical standpoint (**J2**). In their typical form, point-process models are not disaggregators *per-se* but weather generators. Koutsoyiannis

and Onof [2001] presents a point-process model coupled with an iterative adjustment procedure, which enables the use of the model as a disaggregator, and has indeed seen wide use in the field of urban hydrology [Hanaish et al., 2011, Debele et al., 2007, Pui et al., 2012, Villani et al., 2015]. A different approach is that of multiplicative cascades, which are based on the scale invariance of rainfall. Their inspiration comes from cascade models of turbulence [Mandelbrot, 1974, Yaglom, 1966], and while the exact nature of the turbulence-rainfall relationship is unknown, multiple studies have supported the existence of scaling in spatial and temporal rainfall [Schertzer and Lovejoy, 1987, Tessier et al., 1996, Olsson, 1995a, Hubert et al., 1993, Harris et al., 1996] (**J2**). Multifractal scaling implies that the statistical moments of the data are related to the spatial (and/or temporal) scale via a power-law. In their discrete form, cascade models subdivide an initial mass to successive subintervals in a multiplicative manner [Molnar and Burlando, 2005]. A distinction is made between *canonical* and *microcanonical* models, the former of which only preserves mass on average, while the latter does so exactly. The main difference between individual models (of both types) is the choice of probability distribution used to perform the scale-by-scale redistribution of mass. Multifractal disaggregators have been developed in various flavours for the disaggregation of spatial rainfall, typically [Gupta and Waymire, 1993, Over and Gupta, 1994, Schertzer and Lovejoy, 1987, Menabde et al., 1999] but not exclusively [Müller and Haberlandt, 2015] to do with radar images, as well as temporal rainfall [Molnar and Burlando, 2005, Hingray and Haha, 2005, Licznar et al., 2011a, Pui et al., 2012, Onof et al., 2005, Sivakumar and Sharma, 2008, Olsson, 1995b, Pathirana et al., 2003, Serinaldi, 2010, Menabde and Sivapalan, 2000, Olsson, 1998, Olsson and Berndtsson, 1998, Güntner et al., 2001, Menabde et al., 1997, Rupp et al., 2009, Licznar et al., 2011c, 2015], mostly to do with urban hydrology applications (using gauges), and finally in the spatio-temporal domain [Over and Gupta, 1996, Deidda, 2000, Deidda et al., 1999, 2006, Veneziano et al., 2006]. A non-parametric alternative to the two aforementioned approaches is the method of fragments, which is a relatively new procedure, based on resampling a vector of ratios of sub-daily to daily rainfall, typically via a modified k-nearest neighbours algorithm [Lall and Sharma, 1996]. The method of fragments has been employed for urban hydrology applications using gauge data [Sharma et al., 2006, Pui et al., 2012] and also extended to ungauged locations [Westra et al., 2012], with very good performance in both cases.

The point-process disaggregators have been shown to perform adequately for gauge data on a point-by-point basis [Koutsoyiannis and Onof, 2001, Debele et al., 2007, Villani et al., 2015] (**J5**), and have also been extended for disaggregation at unmeasured locations [Cowpertwait et al., 1996, Koutsoyiannis et al., 2003, Gyasi-Agyei and Mahbub, 2007], with some studies also addressing the issue of parameter temporal stationarity in relation to climate change [Burton et al., 2010]. While point process disaggregators appear to be a relatively mature procedure, their parameterisation is not straightforward, as they typically consist of at least 5 parameters (in their most basic form), which are fitted via analytical relations [Rodriguez-Iturbe et al., 1987, 1988], and also do not have an explicit way of dealing with zero rainfalls (thresholding is typically used). The choice of statistics for fitting is somewhat ad-hoc and the procedures used difficult to justify. Some authors have sought to address this via various optimisation

schemes [Onof and Wheater, 1993, Khaliq and Cunnane, 1996, Pui et al., 2012] but this then adds an additional computational burden to what is already a non-straightforward fitting exercise (indeed, some authors note that even with iterative fitting procedures, some local optima may be unobtainable [Pui et al., 2012]). This procedure could be fitted externally from JULES and parameter ancillaries provided, which would satisfy **J3**, but the ambiguous fitting procedure may restrict its application for arbitrary global locations (**J1**, **J2**) While the model fitting can be external to JULES, the adjusting procedure for its use as a disaggregator may still present a large numerical expense (**J4**), as it iteratively modifies the disaggregated time series until its statistics match that of the daily-scale within a chosen error tolerance, the choice of which can be arbitrary (**J2**).

The widespread use of multiplicative cascades (see references above) could be taken as testament of their adequacy, and they are attractive in their simplicity, with only two parameters in their simplest form (**J3**, **J4**). However, there are significant practical considerations to do with the model type and structure. First, a decision between the canonical and microcanonical formulation is needed. As canonical models preserve mass only on average, this implies the need for multiple runs of the disaggregator in order to obtain a forcing that adequately reflects the statistical properties of the calibration data, which is at odds with **J4**, and may also introduce an additional bias in the model water budget, for which closure problems are already an issue [Haddeland et al., 2011] (**J5**). Microcanonical models, though less general in their assumption of explicit conservation of mass, seem preferable for use in JULES from the viewpoint of **J4**, **J5**. The second consideration then, with implications for **J5**, is the choice of statistical approximation for modelling the redistribution of the rainfall to be disaggregated - the so-called *cascade generator* W, defined as the weights that determine the proportions of the coarse-scale rainfall that get redistributed to every disaggregated timestep. The simplest assumption - a uniform W [Olsson, 1998] - has been found to be only narrowly applicable, and the symmetrical beta distribution is the most widely used formulation [Molnar and Burlando, 2005, Pui et al., 2012, and references therein]. The model parameters have been found to be scale-dependent [Menabde et al., 1997, Menabde et al., 1999], and models accounting for this are dubbed *bounded* cascade disaggregators [Menabde and Sivapalan, 2000]. The most complicated cascade procedures incorporate dependence on both scale and rainfall intensity [Rupp et al., 2009, Serinaldi, 2010], or employ complicated mixed distributions [Licznar et al., 2011a,b,c, 2015]. The choice of the exact microcanonical formulation for JULES cannot be done *a priori* and requires an analysis of the data, with due consideration of what is sufficient in terms of **J5**, while keeping in mind any added complexity in the model formulation[1].

Resampling based on the method of fragments would probably be the best choice to satisfy **J5** in an ideal world, as it builds the disaggregated series from fragments of real data, enabling it to most accurately match its statistics, compared to the aforementioned procedures [Pui et al., 2012, note that this is the only such intercomparison study known to us]. However, this method supposes that a sufficiently long high-resolution time series is available for resampling, when the goal of the disaggregator is precisely to avoid this (**J3**). At the scale of a global use case (**J1**), if a sufficiently long sub-daily

[1] As expressed by Aristotle (384-322 BC): *We may assume the superiority, other things being equal, of the demonstration which derives from fewer postulates or hypotheses or propositions* [Posterior Analytics, I, 25]

resolution time series is available and necessary to be present for the method to be employed, then is it not easier to simply use it to drive the model?

From the above, microcanonical cascades seem to be the only procedure that can satisfy **J1**,**J2**,**J3**,**J4**, the question is then one of choosing the right formulation that satisfies **J5** to an acceptable standard, while keeping in mind the model complexity.

2 Methodology

2.1 Choosing a calibration dataset

Before a globally-applicable disaggregator can be implemented, a sufficiently long sub-daily global calibration dataset is needed. For example, the CMORPH dataset combines gauge measurements with satellite data from the TRMM platform at a 3h resolution, but is only quasi-global in coverage [Joyce et al., 2004]. It is theoretically conceivable that a global-scale aggregation of sub-daily gauge records can be assembled, but the quality assurance and data standardisation challenge it presents is beyond the scope of this work. The NASA GPM mission offers a uniquely high-resolution 30-minute global dataset, but only offers data from 2014 onward [Huffman et al., 2013]. Reanalysis data can be used, yet the precipitation products therein may be strongly dominated by the host models' physics schemes, with known limitations in their ability to reproduce precipitation for regions with dominant convective rainfall regimes [Adler et al., 2001, Bosilovich et al., 2008]. However, to the knowledge of this author, they seem to be the only alternative that is both global and at a sub-hourly scale. One such dataset is WFDEI - the WATCH Forcing Data methodology applied to ERA-Interim data [Weedon et al., 2014]. This dataset is chosen due to its sufficient spatio-temporal coverage, but also because it is already familiar within the JULES community (e.g. Warszawski et al. [2014]). With regards to comparing the disaggregated outputs to real-world (e.g. gauge) precipitation, the error introduced by the disaggregator would be in addition to the error already present in WFDEI. However, as the latter is already known to the modelling community, disentangling the effects of the former would be easier.

The WFDEI-GPCC dataset is chosen (i.e. bias-corrected using GPCC measurements) due to the reasons outlined in Weedon et al. [2014]. The data is at 0.5°spatial and 3-hourly temporal resolution and spans 1979-2010, with rainfall and snowfall rate products provided separately. At this preliminary stage, the analysis was performed only for the rainfall rate product[2] (kg/m^2s), which was converted to a 3-hourly rainfall accumulation ($mm/3h$). In order to perform a global-scale analysis but circumvent the large computational time required for processing the entire 0.5°x0.5°model grid, we adopted the regional classification scheme of Giorgi and Francisco [2000]. Within each Giorgi region in Figure 1, 3% of the area, as defined by the bounding box of each region, was sampled, which yielded a total of $\sim$3000 points. This was found to be both a reasonable sample in terms of global coverage and small enough so as not to take overly long to compute. As Giorgi and Francisco [2000] exclude the northern-most

[2]It is pertinent to note that to the knowledge of this author, no studies in the disaggregation literature address the explicit disaggregation of snow.

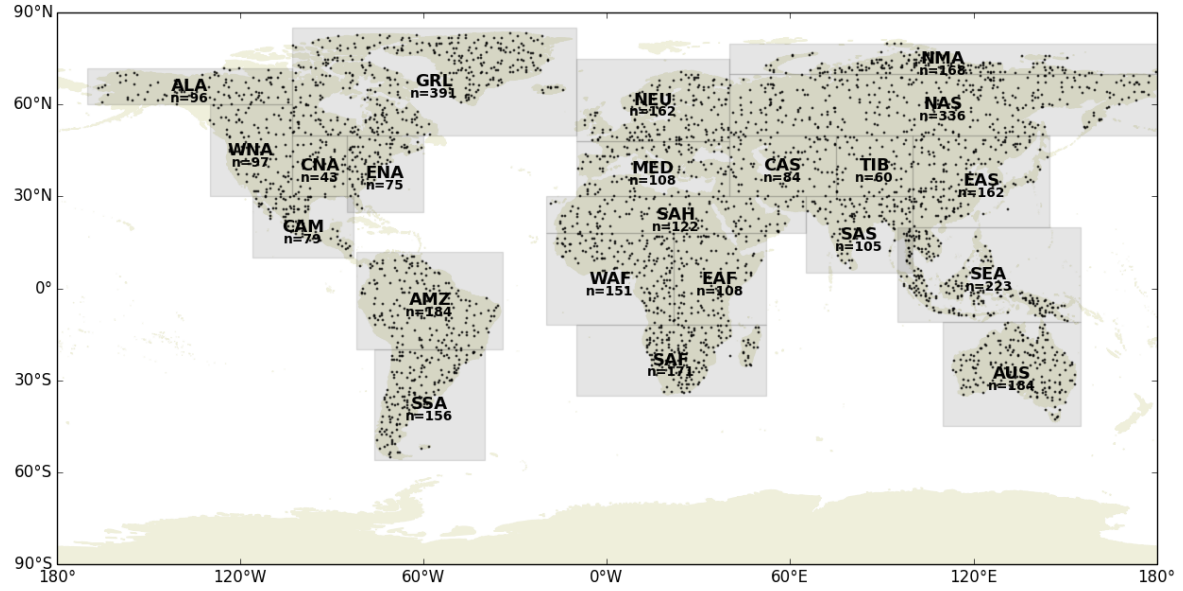

Figure 1: Map of sampled points for this analysis within each Giorgi region. For abbreviations, see Giorgi and Francisco [2000]

part of Russia, we included this as region "NMA" (Northern-most Asia) for the sake of completeness. Note that under the regional definitions of Giorgi and Francisco [2000] there is a slight overlap between regions SAS and SEA. This does not mean that the points therein have been included in the analysis twice, it simply makes it ambiguous as to which region they belong to.

2.2 Cascade model formulation

Starting from scale $n = 0$, a discrete microcanonical multiplicative cascade procedure distributes the quantity (mass of rainfall in our case) to be disaggregated to successively smaller subdivisions with a branching number b. We use the most parsimonious and widely used case, in which the original resolution is halved at each cascade scale n, i.e. $b = 2$. The ith subdivision at level n is denoted $\Delta_{n,i}$, there being $i = 1, ..., b^n$ subdivisions at level n. Distributed mass is then the product of a multiplicative process at all levels n, with the mass of $\Delta_{n,i}$ given as:

$$\mu_n(\Delta_{n,i}) = R_0 \prod_{j-1}^{n} W_j(i) \qquad \text{for } i = 1, 2, ..., b^n; \quad n > 0 \tag{1}$$

R_0 is the initial depth of rainfall at $n = 0$ and W is the cascade generator with $E[W] = 0.5$ and $W\epsilon[0, 1]$. W_j is essentially a weight that determines the portion of R_n that is distributed to $\Delta_{n+1,i}$. As there are b^{n+1} subdivisions at level $n + 1$, the same number of weights must be generated. For a given $\Delta_{n,i}$ timestep, there are two corresponding timesteps $\Delta_{n+1,2i-1}$, $\Delta_{n+1,2i}$, and for mass to be conserved exactly in the redistribution, the corresponding weights $W_j(2i - 1) + W_j(2i) = 1$. W_j then denotes the *distribution* of weights for a transition between two given cascade levels, i.e. j in Equation 1 stands for

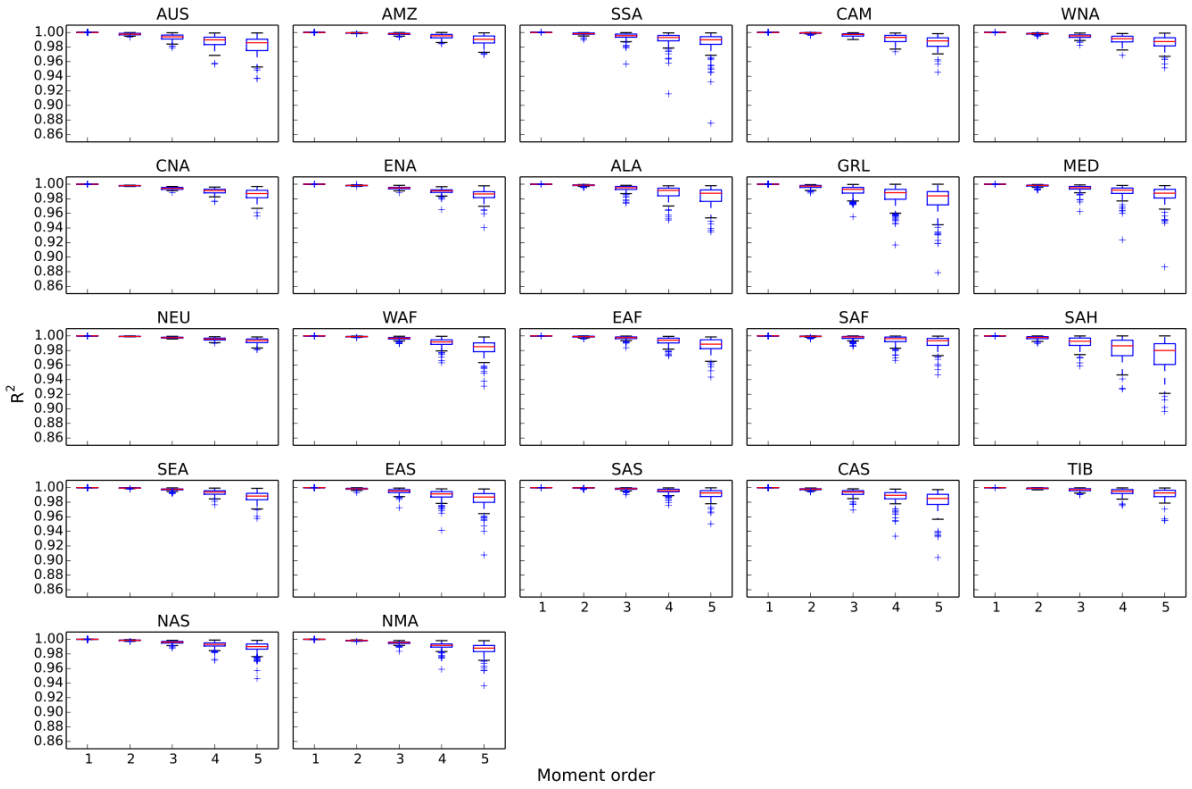

Figure 2: Linear goodness-of-fit for the log-log q-order moment relationships with scale for every Giorgi region. Calculations for each point are separate, these are subsequently aggregated into boxplots. Whiskers are 5th,95th confidence intervals and represent the spread of points within each region. A higher spread simply represents more variability within a region.

$n \rightarrow n+1$. Figure 3 shows a worked example.

For all properties of the cascade to be evaluated, the calibration data at the finest resolution $\lambda_{n_{max}}$ is taken and then aggregated up to successively coarser scales with $b = 2$, i.e. the cascade from Figure 3 is inverted, with every two timesteps at $n+1$ that correspond to n being summed to make up the rainfall volume of R_n at a given timestep. In our case $\lambda_{n_{max}} = \lambda_3 = 3h$

In order for the cascade procedure to be applicable, we need to establish that scaling behaviour indeed exists in the WFDEI rain field. We define the sample moments[3] of the data as:

$$M_n(q) = \sum_{i=1}^{b^n} \mu_n^q(\Delta_{n,i}) \tag{2}$$

$q \geq 1$ being the moment order. In multiplicative cascades, the sample moments should obey a log-log linear relation to the scale of resolution λ_n (e.g.$\lambda_0 = 24h$, $\lambda_1 = 12h$ etc.) (e.g. Olsson [1998]). We examine this for every sampled point and every moment order q by fitting a least-squares regression and evaluating the R^2. Resolutions up to $192h$ are used and moments of integers from 0 to 5. For the remainder of the model formulation and parameterisation, only resolutions up to $24h$ are used, as these

[3]Note that these are related to but different from the mean, variance, etc., which are sample moments *centered around the mean*.

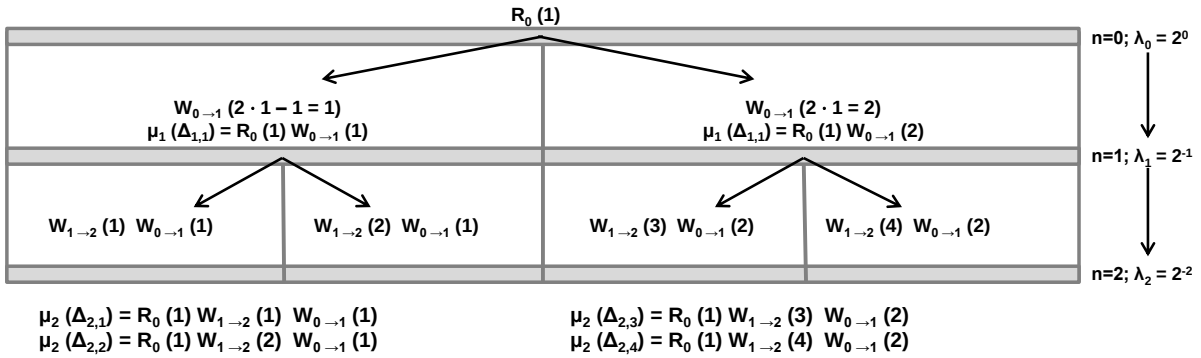

Figure 3: Worked example of a multiplicative cascade with $b = 2$ as per Equation 1.

are the ones of practical interest. It can be seen from Figure 2 that the power-law relation of scale and moments is very well respected. There is more divergence toward higher-order moments, which is a known feature in such analyses, as higher order moments are increasingly strongly dominated by more extreme values [Olsson, 1998]. We do not assess the data's scaling properties any further and instead focus on the practical use and implementation of the cascade procedure. The ERA-Interim precipitation product has been shown to exhibit scaling behaviour [Lovejoy et al., 2012] and since WFDEI-GPCC is based on this, we expect the scaling property to be preserved in our calibration data.

It then remains to be determined what the appropriate distribution for W should be. In a micro-canonical cascade, the distribution of W is identical to that of the "breakdown coefficients", which are simply the proportions of R_n that get redistributed to its two corresponding timesteps at $n + 1$, and are calculated from non-overlapping adjacent pairs of rainfall measurements:

$$W_j(2i-1) = \frac{R_n(i)}{R_{n+1}(2i-1)}; \quad W_j(2i) = \frac{R_n(i)}{R_{n+1}(2i)}; \quad i = 1, ..., N-1 \,\mathrm{for R_n(i)} \neq 0 \tag{3}$$

N being the length of the time series at scale n. Note that W_j is determined only for timesteps at n that have a non-zero rainfall volume, because from the inversion of the cascade, if the corresponding timesteps at $n + 1$ both have zero rainfall volumes, then division by zero would occur in Equation 3. The intermittency and variability of rain are parameterised independently for every scale transition j. The intermittency of rain is determined by the portion of the W_j distribution equal to 0 or 1, while the variability is $W_j \epsilon (0, 1)$. The intermittency parameter $p_{0,j}$ is simply the proportion of $W_j = 0, 1$ to the total number of W_j instances, i.e:

$$P(W_j(2i-1) = 0, 1 \,\mathrm{or}\, W_j(2i) = 0, 1)). \tag{4}$$

The parameterisation of the variability parameter is achieved by using a statistical distribution which allows $E[W] = 0.5$ and $W \epsilon (0, 1)$. We computed the empirical W_j distribution for every WFDEI sample point for scale transitions between 24h to 3h (Figure 4). From this we can see that there is a tendency with increasing resolution toward $W = 0.5$ for all regions. To be able to represent the shape of the

$W\epsilon(0,1)$ distribution, we adopt the symmetrical beta distribution as a first-pass attempt as in Molnar and Burlando [2005], plus also parameterise the model separately at every scale - i.e. a bounded cascade[4]. The symmetrical beta distribution has a single parameter a, which can be parameterised via the method of moments, which is the usual approach in the disaggregation literature (e.g. Pui et al. [2012]):

$$a = \frac{1}{8\mathrm{Var}(W_j)} - 0.5 \tag{5}$$

With the symmetrical beta distribution defined as:

$$f(w) = \frac{1}{B(a)} w^{a-1}(1-w)^{a-1} \tag{6}$$

This distribution satisfies $E(W) = 0.5$ and has a variance $\mathrm{Var}(W)$, where W in this case is only the non-intermittent part of the cascade. The beta distribution has the convenient property of adopting a bell shape for $a > 1$, a U-like shape for $a < 1$ and is identical to the uniform distribution at $a = 1$. In the case of $b = 2$, we need to generate two values of W_j ($W_j(2i-1)$ and $W_j(2i)$) so that $W_j(2i-1) + Wj(2i) = 1$ and are distributed according to Equation 6. For this, we generate two independent gamma-distributed numbers x_1 and x_2 with parameter a. Their ratios $W_j(2i-1) = x_1/(x_1+x_2)$ and $W_j = x_2/(x_1+x_2)$ satisfy both requirements [Menabde and Sivapalan, 2000]. The parameters are estimated using the full time series for every point.

2.3 Model validation

The common way to test the performance of disaggregators is to take the calibration data at the finest resolution $\lambda_{n_{max}}$ and aggregate it to the resolution from which dissaggregation would be performed in the operational case - i.e. in our case $\lambda_{n_3} = 3h$ is aggregated to $\lambda_{n_0} = 24h$. It is then disaggregated back to $3h$ and the distributions are compared. Using the full sample for calibration is the preferred approach in the disaggregation literature, with evaluation then performed via comparison of attributes of the data that are not modelled directly, but reflect the ability of the model to match the properties of the real data [Stedinger and Taylor, 1982]. In our case, we focus on:

- The cumulative distribution of non-zero rainfall. In order to be able to jointly represent the results for every point in every region, we evaluate the performance for the 5th, 25th, 50th, 75th and 95th quantiles
- The variance of the data
- The average annual maximum and its standard deviation
- The lag-1 autocorrelation
- As preliminary analysis showed that the WFDEI data displays a threshold for non-zero rainfall that appears consistently higher than what would be expected for a continuous distribution (which is

[4]Note that in Molnar and Burlando [2005] the dependence of the model parameters with scale is abstracted via a log-log linear relation. In our case, for simplicity, we simply adopt a separate parameterisation at every scale

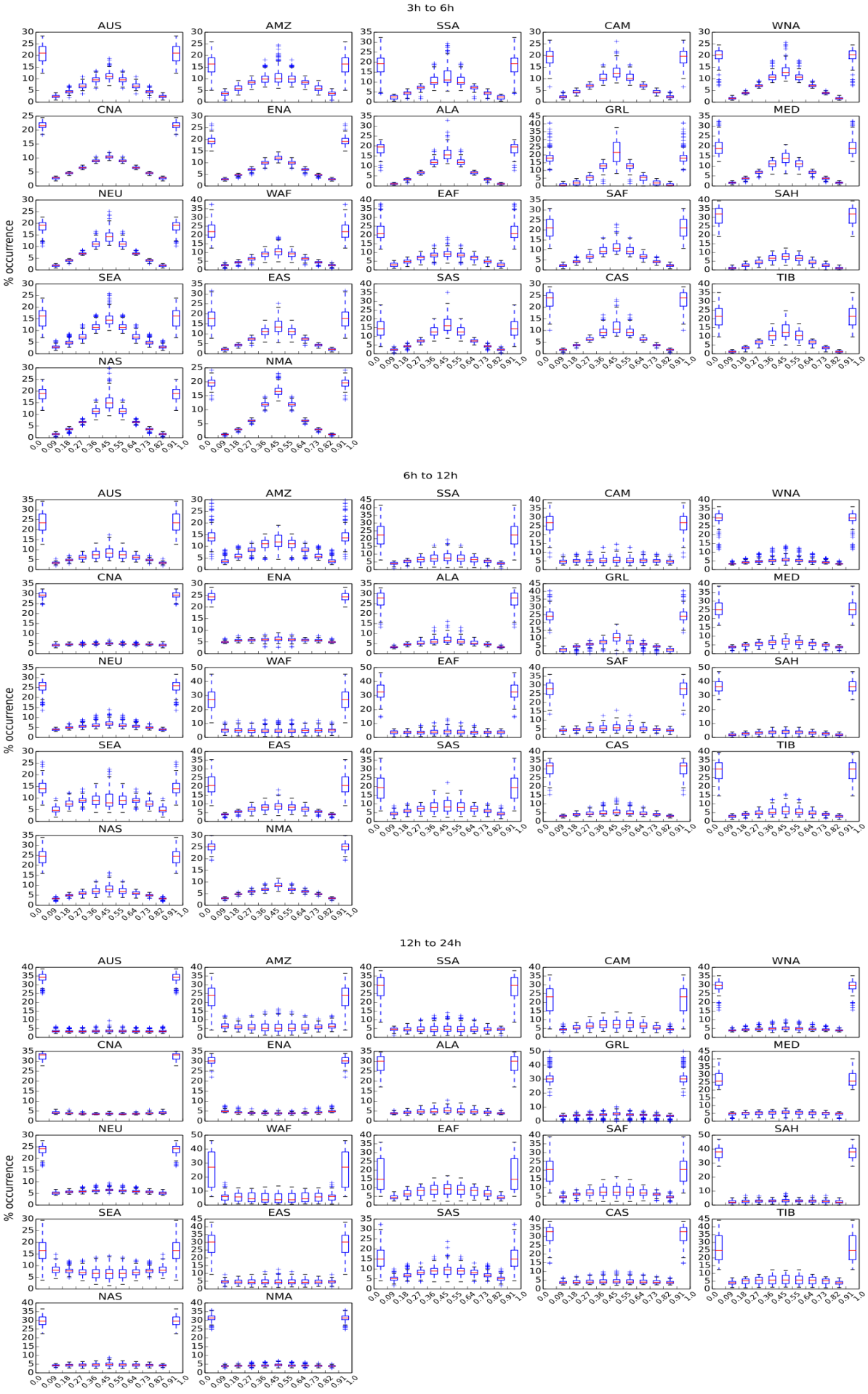

Figure 4: Empirical distributions of W for every sampled WFDEI point within every Giorgi region. Each point distribution was quantised into bins as in the figure and then the individual point value for each bin was aggregated into a boxplot. Whiskers are 5th,95th confidence intervals and represent the spread of points within each region. A higher spread simply represents more variability within a region.

be the case for the disaggregated data), we also evaluate the magnitude of minimum non-zero rainfall

- We evaluate the 5th, 25th, 50th, 75th and 95th quantiles of the distributions of rainfall event lengths (number of $3h$ timesteps) and volumes (mm). An event is defined as a sequence of non-zero timesteps (e.g. Olsson [1998])

Finally, in order to evaluate the performance of the disaggregator W distribution to match that of the data, we generate 100 synthetic distributions with the model parameters at every point, with length $N_j = N_{W_j}$ and evaluate the ensemble averages and standard deviations. N_{W_j} is the number of weights at a given scale transition j. As W_j is defined only for non-zero rainfall at scale n (Equation 3), it corresponds to the the number of non-zero rainfall timesteps at n, and is used as a shorthand for this later in this report. "Ensemble" refers to the statistical aggregation of the individual synthetic runs. Unless otherwise noted, for all analyses, we present the ratio of the disaggregated statistics ($WFDEI_{disagg}$) to that of the original data ($WFDEI$), which gives an indication of the magnitude of over or underestimation of the disaggregator. This is preferred because it allows for easier visualisation, but also because it offers a way to purely compare the relative performance of the model across studies, as comparison of magnitudes would also involve any differences between the WFDEI reanalysis and the station data used in the comparison studies, and is not the goal of this report.

Other studies that look at a bounded microcanonical model based on a beta distribution with a formulation close to ours are those of Molnar and Burlando [2005], Pui et al. [2012], Rupp et al. [2009] and Licznar et al. [2011b]. For these, the target resolution is $10min$ ($n = 7$), $1h$ ($n = 3$), $1h$ ($n = 5$) and $5min$ ($n = 8$) respectively. When disaggregating from a daily or quasi-daily accumulation (as is needed if the resolution at n_{max} does not allow aggregation to exactly $24h$), $n = 3$ is roughly equivalent to $3h$. As will be revealed in the next section,the mismatch between the modelled and empirical distributions of W increases with resolution and thus n. We expect the ratio of mismatch in the model to propagate as n increases comparatively between studies, regardless of the calibration data's original resolution and the target scale, as it is a product of the mismatch of the multiplicative weighting as the scale increases. Thus, focusing on $n = 3$ allows us to compare these studies with ours. Of these studies, Molnar and Burlando and Licznar et al. fall within NEU, while Pui et al. and Rupp et al. are within AUS. We will refer to these studies where the same or similar statistics are studied. We use WebPlotDigitizer [Rohatgi, 2014] for digitising the figures from these studies referred to in this document. As no graphics digitising software is perfect, all numbers cited are approximate.

3 Results

3.1 The disaggregator distribution

Figure 5 shows the average performance of the disaggregator for matching the empirical W distribution, while Figure 6 shows the standard deviation between ensemble runs. For $W = 0, 1$, as governed by

the intermittency parameter p_0, we can see that the standard deviation between disaggregated runs is consistently very close to zero (Figure 6) and that it is reproduced very close to 1:1 across all regions (Figure 5). As p_0 is explicitly set to the probability of $W = 0, 1$ in the calibration data (Equation 4) for every scale, we expect this to be reproduced 1:1. However, for $W\epsilon(0, 1)$ according to Equation 6 (Figure 5), we see that while at the $24h$ resolution the distribution is generally matched well, there is a tendency for underestimation of $W = 0.5$, which strengthens with increasing resolution. It can be seen that the disaggregator generally underestimates toward the centre of the distribution and overestimates towards the tails with the exception of $W = 0.1, 0.9$. Looking at the standard deviations, these are noticeably high for regions GRL (Greenland), SAH (Sahara) and to slightly lesser extents SSA (Southern South America) and the Mediterranean (MED). These regions are all arid regions (especially GRL and SAH, but also true for certain areas of SSA and MED) with rare instances of rainfall and thus a low number of W instances. When generating a W approximation via Equation 6 with a given a value and $N = N_W$, we would expect a convergence toward a stable shape as $N_W \rightarrow \infty$. With a low N_W, we can thus expect considerable variability between ensemble members, which explains the large standard deviations observed. This also explains the very large (e.g. up to 14x for GRL) overestimations in Figure 5 - with only a limited N_W for a given point, we can expect certain bins to be nigh-empty, but this cannot be accounted for by a continuous distribution, so overestimation is observed. This mismatch of the empirical distribution will have implications for the rest of the results, discussed below. There is a possibility that the result for GRL at least is due to the fact that the bulk of the precipitation in that region is in the form of snow, which is a separate WFDEI product and not under analysis, though we have not examined this.

Figure 5: Ratio of the ensemble average W for the disaggregator to that of the empirical distribution. The distributions for every point were quantised into bins, calculations carried out separately and aggregated into boxplots. Whiskers are 5th,95th confidence intervals and represent the spread of points within each region. A higher spread simply represents more variability within a region. A value above 1 implies overestimation of the empirical statistic.

Figure 6: Standard deviation of the ratio of the ensemble W to that of the empirical distribution. The distributions for every point were quantised into bins, calculations carried out separately and aggregated into boxplots. Whiskers are 5th,95th confidence intervals and represent the spread of points within each region. A higher spread simply represents more variability within a region.

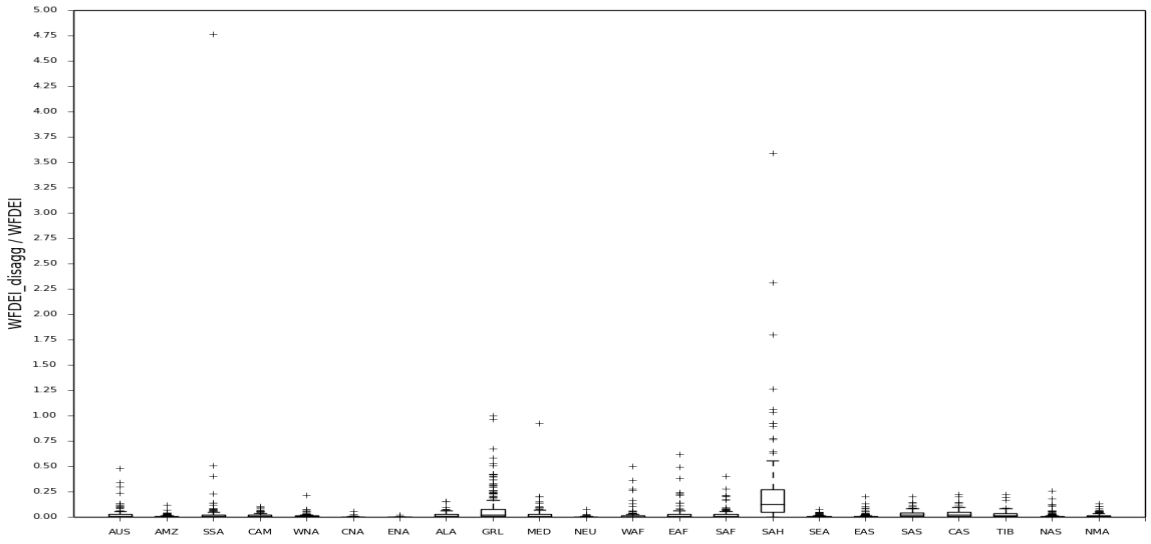

Figure 7: Ratio of minimum non-zero rainfall of the disaggregator to that of the empirical distribution for resolution $3h$. Calculations carried out separately for every point and aggregated into boxplots. Whiskers are 5th,95th confidence intervals and represent the spread of points within each region. A higher spread simply represents more variability within a region.

It is evident that the high variability of the model in very dry areas could pose an operational issue. A way to circumvent this would be to introduce a cross-validation procedure in the generation of the model parameter ancillaries for ultimate use in JULES. An iterated leave-out procedure can be used to test the robustness of the parameter estimates at every point. With an appropriately-defined threshold of acceptable variability, the parameters at points below this threshold can either be set to those of a random adjacent point or their average. Alternatively, the disaggregator in this form can simply be switched off and the uniform disaggregation procedure currently existing in JULES (`precip_disagg_method = 4`) used for these points.

For the rest of the analysis, only figures for resolution $\lambda_{n=3} = 3h$ are shown. The general pattern of increasing magnitude of mismatch with resolution in the analysed statistics reflects that of W.

3.2 Minimum non-zero rainfall

Exploratory analysis revealed that the WFDEI data seems to exhibit a thresholding of non-zero rainfall magnitudes, and our overall analysis in Figure 7 supports this. For all regions, the disaggregator strongly underestimates the rainfall threshold of WFDEI, which is expected as it is governed by a continuous distribution. Some anomalous points exist for SAH and SSA with overestimations, which may be because the particular point is modelled in WFDEI with near-zero rain for the entire 30-year period (some exploratory analysis revealed the presence of at least 1 such point). The WFDEI thresholding would depend on its rain-snow adjustment, gauge catch corrections and monthly total adjustment [Weedon et al., 2011], while in the disaggregator this is stochastic and purely a function of the multiplicative weighting of the initial rainfall at the $24h$ scale. In regions such as SAH, with low number of rainfall

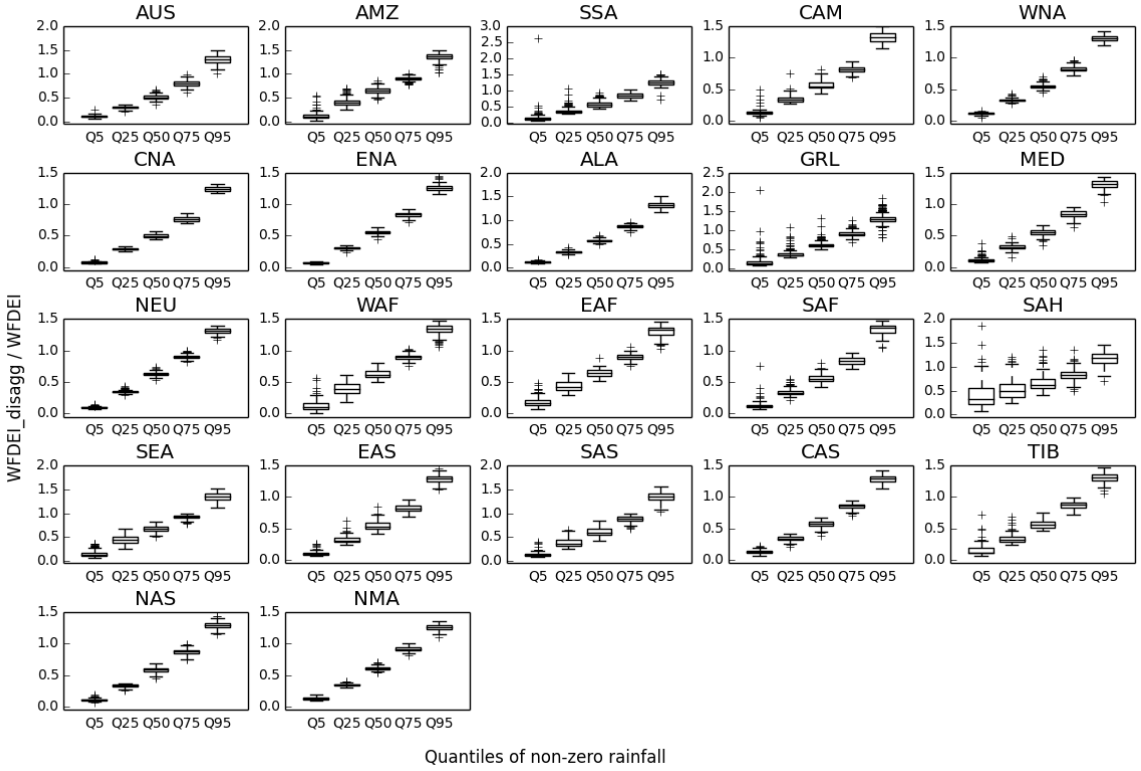

Figure 8: Ratio of quantiles of non-zero rain of the disaggregator to that of the empirical distribution for resolution $3h$. Calculations carried out separately for every point and aggregated into boxplots. Whiskers are 5th,95th confidence intervals and represent the spread of points within each region. A higher spread simply represents more variability within a region.

instances N_W and high probability of zero rain, it is more probable that an initial rainfall volume at $n = 0$ is progressively assigned weights tending toward 0 or 1 as the cascade progresses, thus ultimately yielding a higher value at the $3h$ scale. This may explain the individual instances of overestimation. It is known that disaggregators can produce rainfall minima below those of the calibration data, which is dependent to the accuracy of the measurement instrument (typically gauges). However, this is sometimes dismissed as unimportant in the literature, as most studies are primarily concerned with disaggregation for use in urban hydrology [Molnar and Burlando, 2005]. Obviously, the requirements of the climate modelling community may differ and the issue may need to be addressed. In point-process disaggregators, where zero rainfall cannot be explicitly modelled, the calibration data's threshold is explicitly enforced (e.g. Rodriguez-Iturbe et al. [1988]). However in our case, the problem is not the presence of zeros, the proportion of which is explicitly modelled and preserved (and which a simple thresholding procedure would modify)(Section 3.1). An example fix that would account for the mismatch in thresholding and avoid modifying zeros could be taking the non-zero rainfalls below the threshold of WFDEI and randomly adding them to the timesteps at the lowest quantiles.

3.3 Quantiles of non-zero rainfall

Figure 8 indicates that the model is overestimating the ninety-fifth quantile (Q95) by a factor of $\sim$1.5 across sites, except for SAH, where it is closer to 1:1, plus Q5 is less strongly underestimated than for other regions. As the disaggregator conserves water exactly, an overestimation in one portion of the distribution would need to be made up for by underestimation in another - i.e. the general pattern of overestimation toward Q95 would mean that less rainfall is available to be distributed over lower quantiles, thus underestimating there. Note that the model will preserve the mean of the data exactly, which is in the region of $>\sim$Q75, as is expected for a right-skewed distribution. The mismatch in thresholding from Section 3.3 would lead to allocating more rainfall volume to the lowest-most quantiles, as the disaggregator would be generating more smaller values, but it was found (not shown) that the volume mismatch introduced between zero and the WFDEI threshold is too low (in the range of a few mm at most) to have contributed to the observed pattern of mismatch toward higher quantiles in any significant magnitude. However, it may partially be offsetting the effect of overestimation at higher quantiles for very dry points such as in SAH, which may explain the individual instances of overestimation of Q5 there.

Molnar and Burlando [2005] find that their bounded microcanonical cascade also displays overestimation for most of the CDF and nearing a factor of 2 towards the highest quantiles (Figure 5 in their paper). However, a similar underestimation of the median and below does not occur. They display the data for $n = 7$, so we expect that the result for $n = 3$ would be a somewhat lower mismatch and closer to our observed value. Rupp et al. [2009] also find a factor of ~ 2 overestimation but for $n = 5$ (Figure 13 in their paper). Licznar et al. [2011b] however report an underestimation of ~ 0.6 toward the highest quantiles (Figure 9 in their paper). We suspect this is due to the excess of $W = 0.5$ at the $5min$ resolution for which their results are presented - while the beta distribution underestimates $W = 0.5$, it also overestimates W for the shoulders, thus yielding an overall underestimation at $5min$. For $n = 3$, we can see that the pattern of mismatch is more similar to ours, so we could expect overestimation in that case, but are unable to verify this due to insufficient information presented in the paper (Figure 4 in Licznar et al.).

3.4 Variance

Figure 9 shows a median factor of $\sim$2 overestimation in the disaggregated statistic across regions. The failure of the model to account for the probability density toward $W = 0.5$ (Figure 5), i.e. the centre of the distribution (Equation 6) implies a higher probability density toward the tails, which translates into a higher variance. Even with taking into account the spread around the median, very few points have variances close to 1:1. Pui et al. [2012] find a similar mismatch in the beta distribution at $n = 3$ and corresponding factor of $\sim$2 mismatch in the variance for four points in AUS.

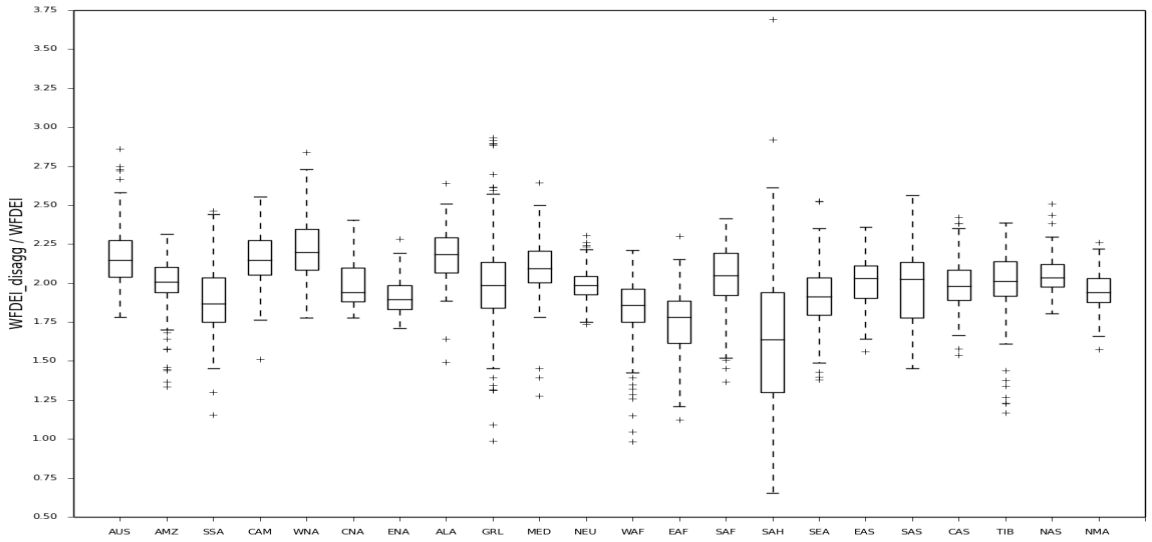

Figure 9: Ratio of variance of the disaggregator to that of the empirical distribution for resolution $3h$. Calculations carried out separately for every point and aggregated into boxplots. Whiskers are 5th,95th confidence intervals and represent the spread of points within each region. A higher spread simply represents more variability within a region.

3.5 Annual maxima

Mean annual maxima and their standard deviations are overestimated by a median factor of near 2 across regions (Figure 10, Figure 11). Pui et al. [2012] examine the intensity-frequency behaviour of their model and find significant overestimation of maxima, which is explained by a similar mismatch of the beta distribution observed and consequent inflated variance, meaning a lower probability of W toward the centre of the distribution compared to the calibration data, thus a higher probability of allocating larger rainfall volumes to individual timesteps at the target scale. At a scale of $\sim 3h$ Molnar and Burlando [2005] show inflation of maxima by a factor of ~ 1.3, somewhat close to our median estimate of ~ 1.8 and within the range of variation for the region. The standard deviation however is underestimated by a factor of ~ 0.6, while for us it is overestimated close to 2x for NEU. However, the annual maxima and standard deviations at $n = 3$ are reproduced close to 1:1 in Licznar et al. [2011b]. This does not fall within the range of values observed for NEU maxima and is only within the tail end of the observed values for standard deviations. Evidently, there can be large variability even with a region as defined in Figure 1 and is it unknown why a discrepancy in the model performance is observed both between studies and compared to our model.

3.6 Lag-1 autocorrelation

Our model is not explicitly formulated in a way that would preserve the autocorrelation of the data. However, Molnar and Burlando [2005] point out that cascade models should preserve a degree of serial correlation due to the nature of the cascade process. Our model underestimates lag-1 autocorrelation by a median factor of 0.25 across regions (Figure 12), with noticeable exceptions for individual points in

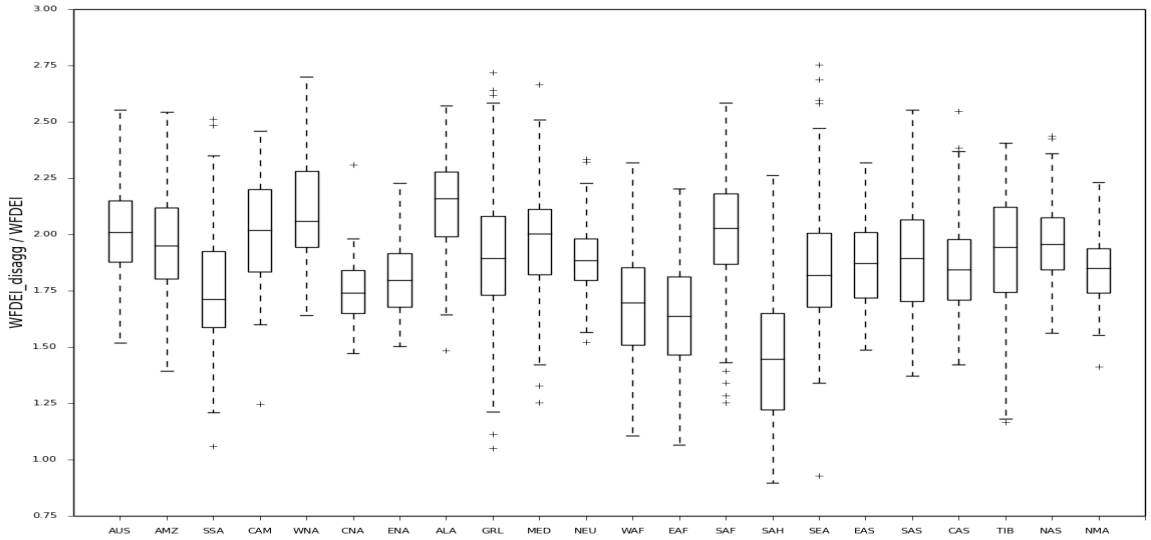

Figure 10: Ratio of average annual maxima of the disaggregator to those of the empirical distribution for resolution $3h$. Calculations carried out separately for every point and aggregated into boxplots. Whiskers are 5th,95th confidence intervals and represent the spread of points within each region. A higher spread simply represents more variability within a region.

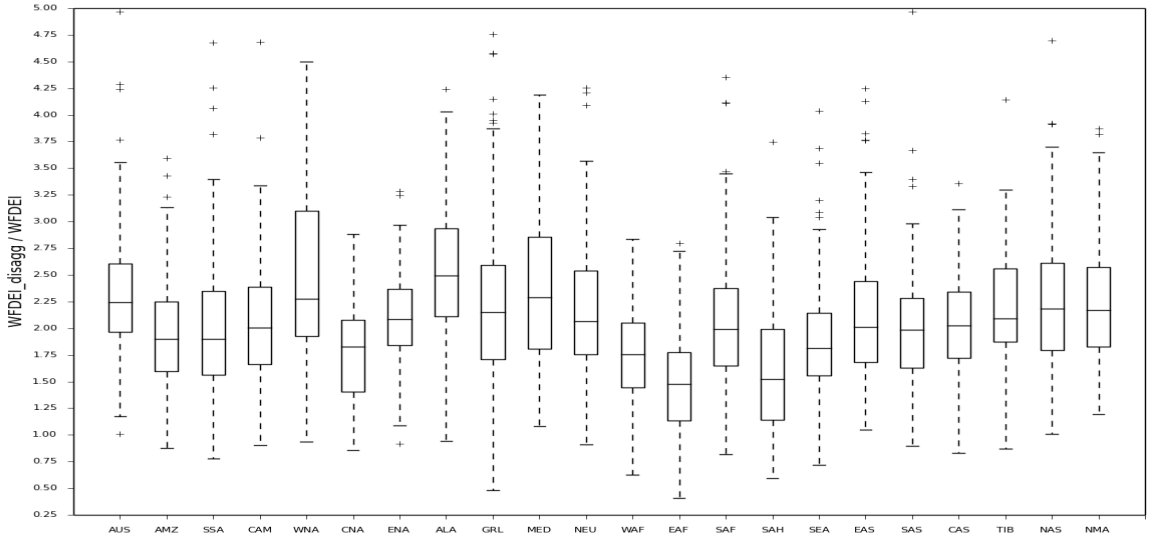

Figure 11: Ratio of annual maxima standard deviations of the disaggregator to those of the empirical distribution for resolution $3h$. Calculations carried out separately for every point and aggregated into boxplots. Whiskers are 5th,95th confidence intervals and represent the spread of points within each region. A higher spread simply represents more variability within a region.

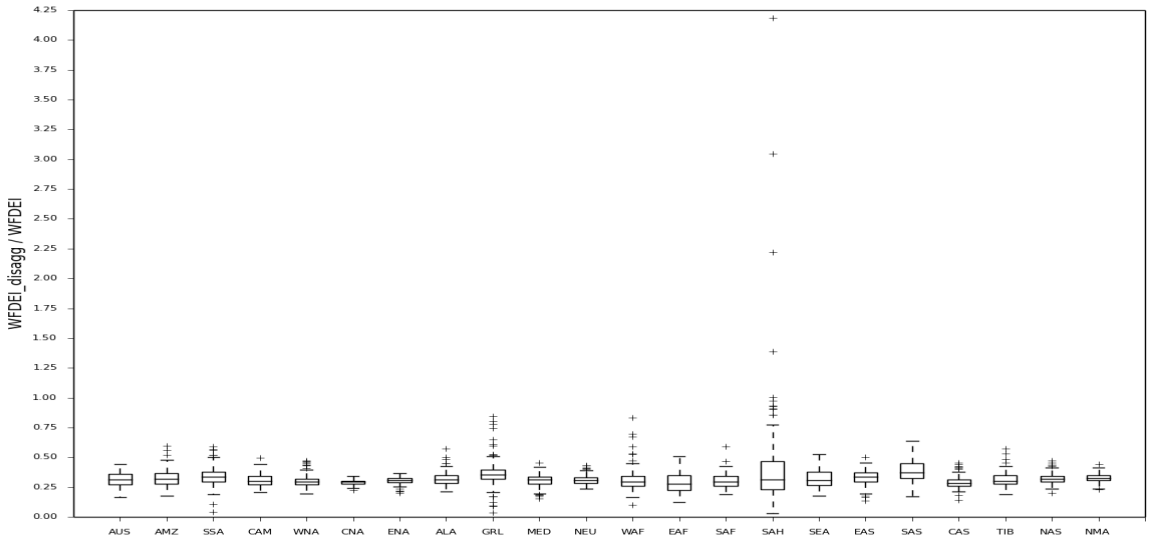

Figure 12: Ratio of lag-1 autocorrelation of the disaggregator to that of the empirical distribution for resolution $3h$. Calculations carried out separately for every point and aggregated into boxplots. Whiskers are 5th,95th confidence intervals and represent the spread of points within each region. A higher spread simply represents more variability within a region.

SAH, which we again attribute to the low number of rainy instances, which gives a higher chance for the disaggregated series to display a pattern that is more persistent than that of the original. In comparison, the factor of underestimation in Pui et al. [2012] is 0.6 for AUS (Figure 9 in their paper), outside the range of values we have obtained. The lag-1 underestimation for Rupp et al. [2009] is a factor of ~ 0.5, also not in the range of values we have observed. Thus, the general fact that our model underestimates the lag-1 autocorrelation is as expected of a cascade procedure, but we are unsure why our result is not in the range of those from the literature, be as it may that the sample to which we compare is essentially of 5 points. Of potential importance for use in JULES, it should be noted that this result means that, for example, the diurnal cycle of the data is not necessarily preserved.

3.7 Rainfall events

For the distribution of individual rainfall event lengths, we see that the shortest event lengths (Q5) are reproduced 1:1 across all regions, with a single exception for a point in AMZ.

For Rupp et al. [2009], the results for underestimation of quantiles Q5 to Q95 are factors of 0.77, 0.61, 0.37, 0.35 and 0.39 respectively, though for $n = 5$. Our results compare favourably, as the lowest factor of underestimation for AUS is ~ 0.4, the median across regions roughly 0.6 (Figure 13). Under the assumption of deterioration of results with increasing n, we may tentatively suppose that the values of Rupp et al. for $n = 3$ would be in the same range as the ones we report. We can compare this to the somewhat different model of Olsson [1998], who also finds underestimation of longer events at $n = 4$, plus underestimated autocorrelation. Event lengths will depend on the intermittency parameter p_0, as it governs the occurrence of zero values in the time series, which terminate an "event". We

have seen that p_0 is preserved (Section 3.1, Figure 5), yet the model still fails to reproduce the full distribution of event lengths, which implies that this is to do with the stochastic nature of the cascade process. We have seen that the lag-1 autocorrelation is underestimated (Section 3.6, Figure 12), thus the seriality of the data is not preserved, and it is then not surprising that the lengths of sequences of non-zero values are not captured for longer sequences. It is noteworthy however that some points actually display overestimations, mostly for median events and above but not exclusively (e.g. a point in SAS).

The underestimation of event lengths implies that too many individual "storms" are generated. With explicit conservation of mass, spreading the rainfall volume from $n = 0$ over more storms than in the original data should result in smaller (underestimated) individual event volumes. From Figure 14, if we look at the median across regions, the underestimation factor roughly ~ 0.7, comparable to that for lengths Olsson [1998]. However, in some regions e.g. SEA, SAS it is actually close to 1:1. The underestimation for volumes however is not so consistent for some regions, with practically all regions displaying at least some points with overestimation, up to 4x in AMZ for example. We suspect that the pattern of mismatch of individual timestep magnitudes from Section 3.3 contributes to this, as it is expected that timesteps with larger volumes would contribute disproportionately more to an event volume, so it then becomes possible for overestimations as those observed to occur. The smallest event quantiles would be thus composed of almost exclusively smaller-magnitude timesteps, which can explain their stronger underestimation, as lower timestep magnitude quantiles are also underestimated.

4 Discussion

If we are to summarise, it appears that our disaggregator's performance is of mostly, though not completely, similar performance compared to the literature, keeping in mind the spatially limited sample therein. As the model is only governed by the distribution of W at every scale, most discrepancies ultimately stem from there. It has been observed that the W distribution for a given interval of rain can be dependent on the state (dry/wet) of its adjacent intervals. Olsson [1998], Güntner et al. [2001] account for this by modelling W for four different interval classes separately. W has also been found to depend on rainfall intensity [Olsson, 1998, Güntner et al., 2001, Veneziano et al., 2006, Rupp et al., 2009, Serinaldi, 2010]. The dependence on magnitude is partially accounted for by Olsson [1998], Güntner et al. [2001] by modelling W separately for intensities above or below the average. Over and Gupta [1994] conditioned W on the intensity of rain at the "mesoscale", which they took as the coverage of a radar frame (for spatial rainfall in their case), but Veneziano et al. [2006] argues that this definition does not have physical or statistical significance, so instead varies the cascade parameters conditional on n. Rupp et al. [2009] takes our version of the microcanonical model and adds a dependence on the intensity of rainfall at $n - 1$. They find that conditioning p_0 alone accounts for most of the discrepancy introduced by the simpler timescale-only dependent beta. Rupp et al. captures these dependencies via fitted relationships, the model having 6 parameters in total, which is a departure from the simple

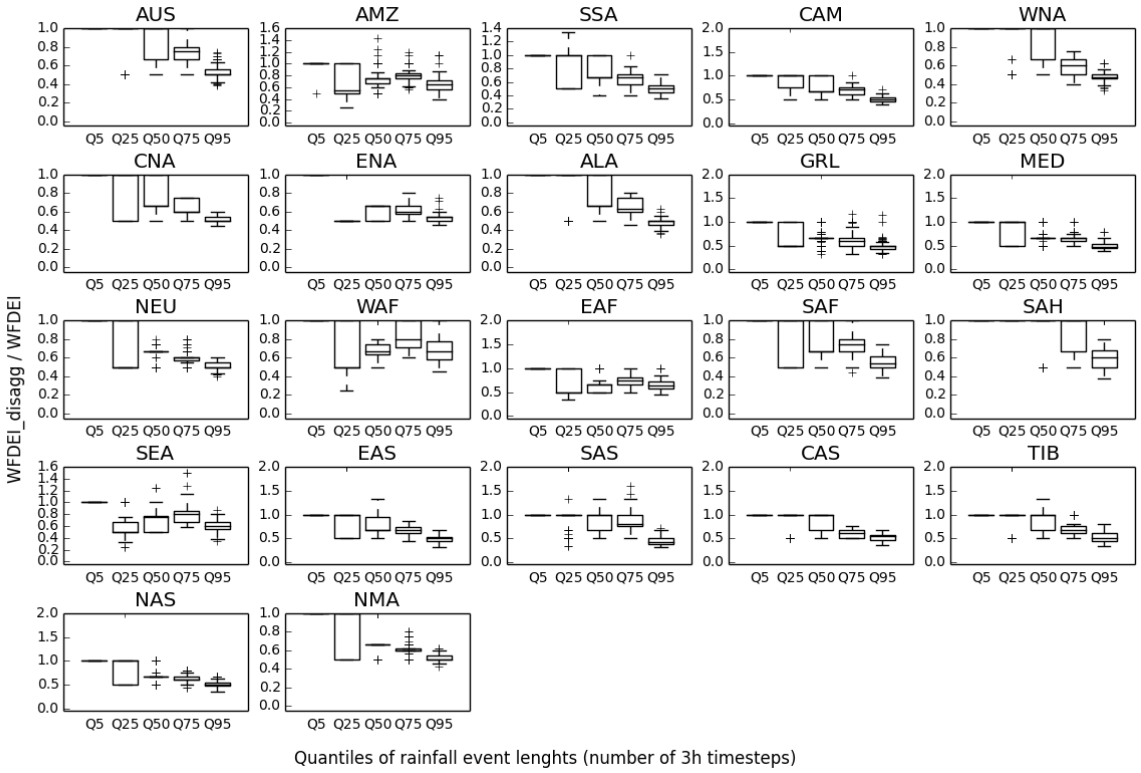

Figure 13: Ratio of quantiles of rainfall events lengths of the disaggregator to that of the empirical distribution for resolution $3h$. Calculations carried out separately for every point and aggregated into boxplots. Whiskers are 5th,95th confidence intervals and represent the spread of points within each region. A higher spread simply represents more variability within a region.

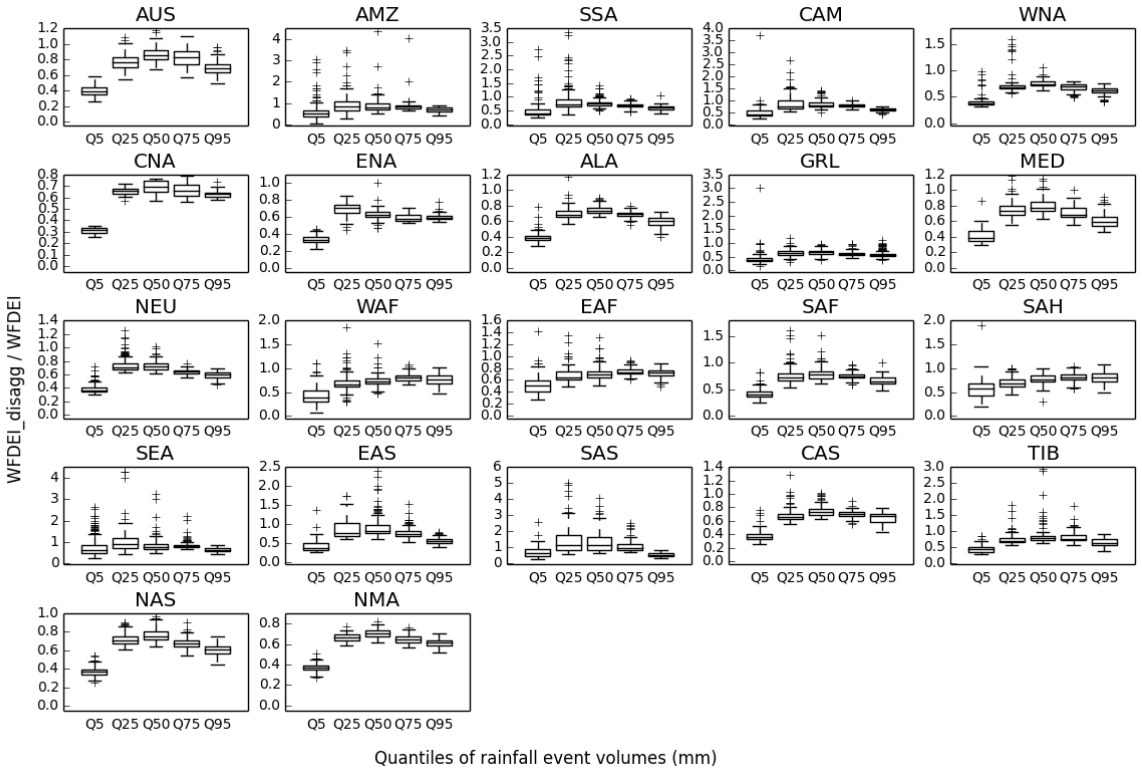

Figure 14: Ratio of quantiles of rainfall event volumes of the disaggregator to that of the empirical distribution for resolution $3h$. Calculations carried out separately for every point and aggregated into boxplots. Whiskers are 5th,95th confidence intervals and represent the spread of points within each region. A higher spread simply represents more variability within a region.

2-parameter (or 4, if we parameterise scale dependence instead of estimating at every n) model used here, but this is also the same amount of models such as Olsson [1998] which however do not account for scale and intensity dependence. Point-process models also have similar amounts of parameters (Section 1) but with substantially more difficult fitting procedures and with need for iterative methods. It is interesting to note that the analysis by Rupp et al. somewhat implies that at least some of the observed dependence on rainfall interval class may be due to the discrete sampling nature imposed by the cascade, where a semicontinuous and irregularly-timed process such as rain is broken up into discrete equally spaced intervals, which may imply that procedures such as Olsson [1998] that explicitly attempt to account for this are unwarranted. However, the dependence on intensity may reflect distinct atmospheric processes, and aggregating these in the analysis of the entire time series may undesirably average-out the parameters [Harris et al., 1997]. Intensity dependence would also capture any seasonal variability, which some authors have accounted for by seasonal parameterisation [Hingray and Haha, 2005]. Serinaldi [2010] manages to introduce more parsimony in the Rupp et al. model by representing both scale and intensity dependence as a single power-law relationship, though its global transferability is unknown.

The authors cited prior note that the ”physical” basis of these models becomes strained and that they are no longer ”multifractal” in the true sense [Rupp et al., 2009, Serinaldi, 2010]. However, they registered improved representation of statistics such as wet/dry spells, autocorrelation and the reproduction of the CDF. [Veneziano et al., 2006] argues that if these models can account for the observed departures from multifractality in the data, and can produce time series that are irregular and ”rain-like” enough, though not necessarily truly multifractal, then they may have utility in the operational case. In the JULES use case, but as well in any model, a physical basis is preferred (**J2**), so then it remains to be determined what the acceptable trade-off between this and reproduction of the rainfall statistics is (**J5**).

4.1 Potential future work

The single most important item of further work is an analysis of the performance of JULES when run with the disaggregated data, as it will review whether more complicated model iterations are required, as discussed above.

We have performed a very limited analysis of the scaling behaviour of the WFDEI-GPCC data. It is known that ERA-Interim displays global scaling behaviour for scales up to approximately 5 days [Lovejoy et al., 2012], so we expect similar performance for WFDEI-GPCC. However, future work can explicitly assess this. Analysing the data’s conservation exponent H would elucidate whether our $a - priori$ microcanonical assumption is empirically valid, as Lovejoy et al. [2012] actually find that $H \neq 0$, which rules out models based on pure multiplicative cascades, such as the microcanonical formulation. Establishing the temporal effective outer scale of the cascade in WFDEI-GPCC would give us a bound for the applicability of a multiplicative cascade disaggregator. Comparing this and the fractal codimension (a measure of the intermittency near the mean) to the results from Lovejoy et al. [2012] can show whether

the addition of WATCH de-biasing to ERA-Interim improves the match in scaling properties as compared to observations, which is a separate issue from this project, but nevertheless interesting. What is more, comparing the empirical and modelled scaling properties of the data allows for identification of any discrepancies in the scaling behaviour, which can inform the adoption of model formulations such as those of Rupp et al. [2009], Serinaldi [2010].

Finally, the JULES use case also encompasses impact studies in the climate change future. Rainfall patterns and their intensity are expected to change with rising global temperatures, yet our disaggregator (and the vast majority of disaggregators in the literature) are temporally stationary - their parameters only reflect the rainfall within the calibration set. For use in multiplicative cascades, two studies are known to this author that seek to address this stationarity. Lisniak et al. [2012] attempt to address this by an additional layer of classification for the cascade generator W, with separate parameterisations of its probability of occurrence for each class. These classes are based on circulation patterns, which are objectively classified using reanalysis data for large-scale atmospheric properties (relative humidity at different pressure levels and vorticity at 850hPa in their case). The dependence of W on the circulation pattern is assumed stationary, but in a GCM case, the change in relative frequency of occurrence of the different circulation patterns then changes the relative frequency in which every parameterisation of W is used. Thus, different types of rainfall events, as classified, would occur more or less often depending on how the large-scale atmospheric properties change in the GCM run. However, Lisniak et al. do not actually find an improvement in their model, but rather take a lack of deterioration in their results with this added degree of freedom as satisfactory. This approach also has operational implications, as adding more classification classes means binning the data into more categories. Parameter estimation would become increasingly difficult with a decrease in timesteps in a class, as is already the case in our model for dry areas (Section 3.1).

A different approach is that of Bürger et al. [2014], who propose a proof-of-concept approach for incorporating the influence of temperature on rainfall extremes from the Clausius-Clapeyron relation by modifying the model probability of intermittency (p_0). They incorporate a temperature dependence via a sigmoid function with two fitted parameters. In the limited scope of their study, they report good results. However, their study implicitly assumes future relative humidity is roughly representative of that currently. They also do not provide a fitting procedure, but rather use a trial-and-error approach within the scope of their paper, with the fitting of the sigmoid being separate to that of the cascade, though it would be preferable if these are jointly fitted. Further still, only p_0 is modified, though if there is also a potential future change in the variability of rainfall, this is not accounted for. Finally, the authors themselves note that their model is in a ”rather arbitrary state” and requires further refinement, e.g. for use in impact studies. Neither approach has seen any follow-up in the literature so far.

5 Conclusion

This document presents a preliminary evaluation of a disaggregator based on multiplicative cascades for the WFDEI-GPCC rainfall (and not snowfall) product, disaggregating $24h$ rainfall accumulations to a $3h$ resolution with explicit conservation of mass. The model is parsimonious, as it is based on only two parameters, governing the intermittency and variability of rainfall. These parameters are estimated separately at every scale of the cascade process. The intermittency of rainfall is estimated directly from the data, while the variability is parameterised via a symmetrical beta distribution. Analysis was performed for regional subsamples of the WFDEI-GPCC grid for disaggregating its entire 30-year rainfall record.

The disaggregator overestimates larger magnitudes in the CDF of empirical rainfall and underestimates lower magnitudes. The variance, and annual maxima of the data are overestimated, the lag-1 autocorrelation underestimated. Shorter rainfall event lengths are generally reproduced but longer events are underestimated. Rainfall event volumes are generally underestimated but this is not necessarily consistent for every analysed point, with overestimations also possible. The general mismatch of the model statistics with those of the calibration data is linked to the failure of the beta distribution to account for the probability density toward the centre of the empirical intermittency distribution, though some discrepancy may also be introduced due to the nature of the random cascade formulation. Overall, the model's performance is roughly similar to that of a limited number of studies known to us that use a similar formulation, though we find that the performance at least for standard deviations of annual maxima and the lag-1 autocorrelation is outside the range of results from the literature. Some operational issues are identified, such as parameter instability for very dry points in WFDEI, as well as potentially a mismatch in the thresholding of minimum non-zero rainfall. Simple procedures to account for these are briefly outlined.

Areas of further work are discussed, with the most pertinent being an evaluation of the model for use in JULES.

Acknowledgements

We are thankful for the comments of Graham Weedon and Richard Betts whose inputs contributed to the direction of this work, plus for the kind support of fellow Climate Impacts Modelling colleagues Camilla Mathison and Ron Kahana.

References

Robert F Adler, Christopher Kidd, Grant Petty, Mark Morissey, and H Michael Goodman. Intercomparison of global precipitation products: The third precipitation intercomparison project (pip-3). *Bulletin of the American Meteorological Society*, 82(7):1377–1396, 2001.

Michael G Bosilovich, Junye Chen, Franklin R Robertson, and Robert F Adler. Evaluation of global precipitation in reanalyses. *Journal of applied meteorology and climatology*, 47(9):2279–2299, 2008.

G Bürger, M Heistermann, and A Bronstert. Towards subdaily rainfall disaggregation via clausius–clapeyron. *Journal of Hydrometeorology*, 15(3):1303–1311, 2014.

A Burton, HJ Fowler, S Blenkinsop, and CG Kilsby. Downscaling transient climate change using a neyman–scott rectangular pulses stochastic rainfall model. *Journal of Hydrology*, 381(1):18–32, 2010.

P.S.P. Cowpertwait, P.E. O'Connell, A.V. Metcalfe, and J.A. Mawdsley. Stochastic point process modelling of rainfall. ii. regionalisation and disaggregation. *Journal of Hydrology*, 175(1-4):47 – 65, 1996. ISSN 0022-1694. doi: http://dx.doi.org/10.1016/S0022-1694(96)80005-9. URL http://www.sciencedirect.com/science/article/pii/S0022169496800059.

Bekele Debele, R. Srinivasan, and J. Yves Parlange. Accuracy evaluation of weather data generation and disaggregation methods at finer timescales. *Advances in Water Resources*, 30 (5):1286–1300, May 2007. ISSN 03091708. doi: 10.1016/j.advwatres.2006.11.009. URL http://dx.doi.org/10.1016/j.advwatres.2006.11.009.

R. Deidda. Rainfall downscaling in a space-time multifractal framework. *Water Resources Research*, 36(7):1779–1794, 2000. ISSN 1944-7973. doi: 10.1029/2000WR900038. URL http://dx.doi.org/10.1029/2000WR900038.

Roberto Deidda, Roberto Benzi, and Franco Siccardi. Multifractal modeling of anomalous scaling laws in rainfall. 1999.

Roberto Deidda, Maria Grazia Badas, and Enrico Piga. Space–time multifractality of remotely sensed rainfall fields. *Journal of hydrology*, 322(1):2–13, 2006.

Filippo Giorgi and Raquel Francisco. Uncertainties in regional climate change prediction: a regional analysis of ensemble simulations with the hadcm2 coupled aogcm. *Climate Dynamics*, 16(2-3):169–182, 2000.

A. Güntner, J. Olsson, A. Calver, and B. Gannon. Cascade-based disaggregation of continuous rainfall time series: the influence of climate. *Hydrology and Earth System Sciences*, 5(2):145–164, November 2001. doi: 10.5194/hess-5-145-2001. URL http://dx.doi.org/10.5194/hess-5-145-2001.

Vijay K. Gupta and Edward C. Waymire. A Statistical Analysis of Mesoscale Rainfall as a Random Cascade. *J. Appl. Meteor.*, 32(2):251–267, February

1993. doi: 10.1175/1520-0450(1993)032%3C0251:asaomr%3E2.0.co;2. URL http://dx.doi.org/10.1175/1520-0450(1993)032%3C0251:asaomr%3E2.0.co;2.

Yeboah Gyasi-Agyei and S.M. Parvez Bin Mahbub. A stochastic model for daily rainfall disaggregation into fine time scale for a large region. *Journal of Hydrology*, 347(3-4):358 – 370, 2007. ISSN 0022-1694. doi: http://dx.doi.org/10.1016/j.jhydrol.2007.09.047. URL http://www.sciencedirect.com/science/article/pii/S0022169407005239.

Ingjerd Haddeland, Douglas B Clark, Wietse Franssen, Fulco Ludwig, FRANK VOß, Nigel W Arnell, Nathalie Bertrand, Martin Best, Sonja Folwell, Dieter Gerten, et al. Multimodel estimate of the global terrestrial water balance: Setup and first results. *Journal of Hydrometeorology*, 12(5):869–884, 2011.

Ibrahim Suliman Hanaish, Kamarulzaman Ibrahim, and Abdul Aziz Jemain. Daily rainfall disaggregation using hyetos model for peninsular malaysia. *matrix*, 2:1, 2011.

D Harris, A Seed, M Menabde, and G Austin. Factors affecting multiscaling analysis of rainfall time series. *Nonlinear Processes in Geophysics*, 4(3):137–156, 1997.

Daniel Harris, Merab Menabde, Alan Seed, and Geoff Austin. Multifractal characterization of rain fields with a strong orographic influence. *J. Geophys. Res.*, 101(D21):26405–26414, November 1996. doi: 10.1029/96jd01656. URL http://dx.doi.org/10.1029/96jd01656.

B Hingray and M Ben Haha. Statistical performances of various deterministic and stochastic models for rainfall series disaggregation. *Atmospheric research*, 77(1):152–175, 2005.

P. Hubert, Y. Tessier, S. Lovejoy, D. Schertzer, F. Schmitt, P. Ladoy, J. P. Carbonnel, S. Violette, and I. Desurosne. Multifractals and extreme rainfall events. *Geophys. Res. Lett.*, 20(10):931–934, May 1993. doi: 10.1029/93gl01245. URL http://dx.doi.org/10.1029/93gl01245.

George J Huffman, David T Bolvin, Dan Braithwaite, Kuolin Hsu, Robert Joyce, Pingping Xie, and Soo-Hyun Yoo. Nasa global precipitation measurement (gpm) integrated multi-satellite retrievals for gpm (imerg). In *Algorithm theoretical basis document, version 4.1*. NASA, 2013.

Robert J Joyce, John E Janowiak, Phillip A Arkin, and Pingping Xie. Cmorph: A method that produces global precipitation estimates from passive microwave and infrared data at high spatial and temporal resolution. *Journal of Hydrometeorology*, 5(3):487–503, 2004.

M.N. Khaliq and C. Cunnane. Modelling point rainfall occurrences with the modified bartlett-lewis rectangular pulses model. *Journal of Hydrology*, 180(1-4):109–138, 1996. cited By 41.

Demetris Koutsoyiannis and Christian Onof. Rainfall disaggregation using adjusting procedures on a Poisson cluster model. *Journal of Hydrology*, 246(1-4):109–122, June 2001. ISSN 00221694. doi: 10.1016/s0022-1694(01)00363-8. URL http://dx.doi.org/10.1016/s0022-1694(01)00363-8.

Demetris Koutsoyiannis, Christian Onof, and Howard S. Wheater. Multivariate rainfall disaggregation at a fine timescale. *Water Resour. Res.*, 39(7):1173+, July 2003. doi: 10.1029/2002wr001600. URL http://dx.doi.org/10.1029/2002wr001600.

Upmanu Lall and Ashish Sharma. A nearest neighbor bootstrap for resampling hydrologic time series. *Water Resources Research*, 32(3):679–693, 1996. ISSN 1944-7973. doi: 10.1029/95WR02966. URL http://dx.doi.org/10.1029/95WR02966.

P Licznar, C De Michele, and W Adamowski. Precipitation variability within an urban monitoring network via microcanonical cascade generators. *Hydrology and Earth System Sciences*, 19(1):485–506, 2015.

Paweł Licznar, Janusz Łomotowski, and David E. Rupp. Random cascade driven rainfall disaggregation for urban hydrology: An evaluation of six models and a new generator. *Atmospheric Research*, 99(3-4):563–578, March 2011a. ISSN 01698095. doi: 10.1016/j.atmosres.2010.12.014. URL http://dx.doi.org/10.1016/j.atmosres.2010.12.014.

Paweł Licznar, Janusz Łomotowski, and David E Rupp. Random cascade driven rainfall disaggregation for urban hydrology: An evaluation of six models and a new generator. *Atmospheric Research*, 99(3): 563–578, 2011b.

Paweł Licznar, TheoG Schmitt, and DavidE Rupp. Distributions of microcanonical cascade weights of rainfall at small timescales. *Acta Geophysica*, 59(5):1013–1043, April 2011c. ISSN 1895-6572. doi: 10.2478/s11600-011-0014-4. URL http://dx.doi.org/10.2478/s11600-011-0014-4.

D Lisniak, J Franke, and C Bernhofer. Circulation pattern based parameterization of a multiplicative random cascade for disaggregation of daily rainfall under nonstationary climatic conditions. *Hydrology and Earth System Sciences Discussions*, 9:10115–10149, 2012.

S Lovejoy, J Pinel, and D Schertzer. The global space–time cascade structure of precipitation: Satellites, gridded gauges and reanalyses. *Advances in Water Resources*, 45:37–50, 2012.

Benoit B. Mandelbrot. Intermittent turbulence in self-similar cascades: divergence of high moments and dimension of the carrier. *Journal of Fluid Mechanics*, 62(02):331–358, January 1974. ISSN 1469-7645. doi: 10.1017/s0022112074000711. URL http://dx.doi.org/10.1017/s0022112074000711.

M. Menabde, A. Seed, D. Harris, and G. Austin. Multiaffine random field model of rainfall. *Water Resources Research*, 35:509–514, February 1999. doi: 10.1029/1998WR900020.

Merab Menabde and Murugesu Sivapalan. Modeling of rainfall time series and extremes using bounded random cascades and levy-stable distributions. *Water Resour. Res.*, 36(11):3293–3300, November 2000. doi: 10.1029/2000wr900197. URL http://dx.doi.org/10.1029/2000wr900197.

Merab Menabde, Daniel Harris, Alan Seed, Geoff Austin, and David Stow. Multiscaling properties of rainfall and bounded random cascades. *Water Resources Research*, 33(12):2823–2830, 1997. ISSN 1944-7973. doi: 10.1029/97WR02006. URL http://dx.doi.org/10.1029/97WR02006.

Peter Molnar and Paolo Burlando. Preservation of rainfall properties in stochastic disaggregation by a simple random cascade model. *Atmospheric Research*, 77(1-4):137–151, September 2005. ISSN 01698095. doi: 10.1016/j.atmosres.2004.10.024. URL http://dx.doi.org/10.1016/j.atmosres.2004.10.024.

H Müller and U Haberlandt. Temporal rainfall disaggregation with a cascade model: From single-station disaggregation to spatial rainfall. *Journal of Hydrologic Engineering*, page 04015026, 2015.

J. Olsson. Limits and characteristics of the multifractal behaviour of a high-resolution rainfall time series. *Nonlinear Processes in Geophysics*, 2(1):23–29, November 1995a. doi: 10.5194/npg-2-23-1995. URL http://dx.doi.org/10.5194/npg-2-23-1995.

J Olsson. Limits and characteristics of the multifractal behaviour of a high-resolution rainfall time series. *Nonlinear processes in Geophysics*, 2(1):23–29, 1995b.

J. Olsson. Evaluation of a scaling cascade model for temporal rain- fall disaggregation. *Hydrology and Earth System Sciences*, 2(1):19–30, November 1998. doi: 10.5194/hess-2-19-1998. URL http://dx.doi.org/10.5194/hess-2-19-1998.

J. Olsson and R. Berndtsson. Temporal rainfall disaggregration based on scaling properties. *Water Science and Technology*, 37(11):73 – 79, 1998. ISSN 0273-1223. doi: http://dx.doi.org/10.1016/S0273-1223(98)00318-7. URL http://www.sciencedirect.com/science/article/pii/S0273122398003187. Use of Historical Rainfall Series for Hydrological ModellingSelected Proceedings of the Third International Workshop on Rainfall in Urban Areas.

Christian Onof and Howard S. Wheater. Modelling of British rainfall using a random parameter Bartlett-Lewis Rectangular Pulse Model. *Journal of Hydrology*, 149(1-4):67–95, August 1993. ISSN 00221694. doi: 10.1016/0022-1694(93)90100-n. URL http://dx.doi.org/10.1016/0022-1694(93)90100-n.

Christian Onof, John Townend, and Richard Kee. Comparison of two hourly to 5-min rainfall disaggregators. *Atmospheric Research*, 77(14):176 – 187, 2005. ISSN 0169-8095. doi: http://dx.doi.org/10.1016/j.atmosres.2004.10.022. URL http://www.sciencedirect.com/science/article/pii/S0169809505000980. Precipitation in Urban Areas6th International Workshop on Precipitation in Urban Areas.

Thomas M. Over and Vijay K. Gupta. Statistical Analysis of Mesoscale Rainfall: Dependence of a Random Cascade Generator on Large-Scale Forcing. *J. Appl. Meteor.*, 33(12):1526–

1542, December 1994. doi: 10.1175/1520-0450(1994)033%3C1526:saomrd%3E2.0.co;2. URL http://dx.doi.org/10.1175/1520-0450(1994)033%3C1526:saomrd%3E2.0.co;2.

Thomas M. Over and Vijay K. Gupta. A space-time theory of mesoscale rainfall using random cascades. *J. Geophys. Res.*, 101(D21):26319–26331, November 1996. doi: 10.1029/96jd02033. URL http://dx.doi.org/10.1029/96jd02033.

Assela Pathirana, Srikantha Herath, and Tadashi Yamada. Estimating rainfall distributions at high temporal resolutions using a multifractal model. *Hydrology and Earth System Sciences Discussions*, 7 (5):668–679, 2003.

A. Pui, A. Sharma, R. Mehrotra, B. Sivakumar, and E. Jeremiah. A comparison of alternatives for daily to sub-daily rainfall disaggregation. *Journal of Hydrology*, 470-471(0):138 – 157, 2012. ISSN 0022-1694. doi: http://dx.doi.org/10.1016/j.jhydrol.2012.08.041. URL http://www.sciencedirect.com/science/article/pii/S0022169412007202.

I. Rodriguez-Iturbe, D. R. Cox, and Valerie Isham. A point process model for rainfall: Further developments. *Proceedings of the Royal Society of London A: Mathematical, Physical and Engineering Sciences*, 417(1853):283–298, 1988. ISSN 0080-4630. doi: 10.1098/rspa.1988.0061.

Ignacio Rodriguez-Iturbe, DR Cox, and Valerie Isham. Some models for rainfall based on stochastic point processes. In *Proceedings of the Royal Society of London A: Mathematical, Physical and Engineering Sciences*, volume 410, pages 269–288. The Royal Society, 1987.

A Rohatgi. *WebPlotDigitizer*, 2014. http://arohatgi.info/WebPlotDigitizer [Accessed: 12 Oct 2015].

David E. Rupp, Richard F. Keim, Mina Ossiander, Marcela Brugnach, and John S. Selker. Time scale and intensity dependency in multiplicative cascades for temporal rainfall disaggregation. *Water Resour. Res.*, 45(7):W07409+, July 2009. doi: 10.1029/2008wr007321. URL http://dx.doi.org/10.1029/2008wr007321.

Daniel Schertzer and Shaun Lovejoy. Physical modeling and analysis of rain and clouds by anisotropic scaling multiplicative processes. *J. Geophys. Res*, 92(D8):9693–9714, 1987.

F. Serinaldi. Multifractality, imperfect scaling and hydrological properties of rainfall time series simulated by continuous universal multifractal and discrete random cascade models. *Nonlinear Processes in Geophysics*, 17(6):697–714, December 2010. doi: 10.5194/npg-17-697-2010. URL http://dx.doi.org/10.5194/npg-17-697-2010.

Ashish Sharma, Sri Srikanthan, et al. Continuous rainfall simulation: A nonparametric alternative. Conference Design, 2006.

Bellie Sivakumar and Ashish Sharma. A cascade approach to continuous rainfall data generation at point locations. *Stochastic Environmental Research and Risk Assessment*, 22(4):451–459, 2008. ISSN 1436-3240. doi: 10.1007/s00477-007-0145-y. URL http://dx.doi.org/10.1007/s00477-007-0145-y.

Jery R Stedinger and Marshall R Taylor. Synthetic streamflow generation: 1. model verification and validation. *Water resources research*, 18(4):909–918, 1982.

Yves Tessier, Shaun Lovejoy, Pierre Hubert, Daniel Schertzer, and Sean Pecknold. Multifractal analysis and modeling of rainfall and river flows and scaling, causal transfer functions. *J. Geophys. Res.*, 101(D21):26427–26440, November 1996. doi: 10.1029/96jd01799. URL http://dx.doi.org/10.1029/96jd01799.

Daniele Veneziano, Pierluigi Furcolo, and Vito Iacobellis. Imperfect scaling of time and space-time rainfall. *Journal of Hydrology*, 322(1-4):105–119, May 2006. ISSN 00221694. doi: 10.1016/j.jhydrol.2005.02.044. URL http://dx.doi.org/10.1016/j.jhydrol.2005.02.044.

Veronica Villani, Daniela Di Serafino, Rianna Guido, and Paola Mercogliano. Stochastic Models for the Disaggregation of Precipitation Time Series on Sub-Daily Scale: Identication of Parameters by Global Optimization. *Social Science Research Network Working Paper Series*, May 2015. URL http://ssrn.com/abstract=2602889.

Lila Warszawski, Katja Frieler, Veronika Huber, Franziska Piontek, Olivia Serdeczny, and Jacob Schewe. The inter-sectoral impact model intercomparison project (isi-mip): Project framework. *Proceedings of the National Academy of Sciences*, 111(9):3228–3232, 2014. doi: 10.1073/pnas.1312330110. URL http://www.pnas.org/content/111/9/3228.abstract.

GP Weedon, S Gomes, P Viterbo, WJ Shuttleworth, E Blyth, H Österle, JC Adam, Nicolas Bellouin, O Boucher, and M Best. Creation of the watch forcing data and its use to assess global and regional reference crop evaporation over land during the twentieth century. *Journal of Hydrometeorology*, 12 (5):823–848, 2011.

Graham P Weedon, Gianpaolo Balsamo, Nicolas Bellouin, Sandra Gomes, Martin J Best, and Pedro Viterbo. The wfdei meteorological forcing data set: Watch forcing data methodology applied to era-interim reanalysis data. *Water Resources Research*, 50(9):7505–7514, 2014.

Seth Westra, Rajeshwar Mehrotra, Ashish Sharma, and Ratnasingham Srikanthan. Continuous rainfall simulation: 1. a regionalized subdaily disaggregation approach. *Water Resources Research*, 48(1):n/a–n/a, 2012. ISSN 1944-7973. doi: 10.1029/2011WR010489. URL http://dx.doi.org/10.1029/2011WR010489. W01535.

A. M. Yaglom. The Influence of Fluctuations in Energy Dissipation on the Shape of Turbulence Characteristics in the Inertial Interval. *Soviet Physics Doklady*, 11:26+, July 1966. URL http://adsabs.harvard.edu/cgi-bin/nph-bib_query?bibcode=1966SPhD...11...26Y.

Met Office
FitzRoy Road
Exeter
Devon
EX1 3PB
United Kingdom

Produced with the Met Office LaTeX template v3.0.0